

5



Unravelling the future role of internal variability in South Asian near-surface wind speed

Cheng Shen¹, Hui-Shuang Yuan², Zhi-Bo Li¹, Jinling Piao^{3, 4}, Youli Chang², Deliang Chen^{1, 5, *}

- ¹ Regional Climate Group, Department of Earth Sciences, University of Gothenburg, Gothenburg, Sweden
- ² Department of Atmospheric Science, Yunnan University, Kunming, China
- ³ Center for Monsoon System Research, Institute of Atmospheric Physics, Chinese Academy of Sciences, Beijing, China
- ⁴ College of Earth and Planetary Sciences, University of Chinese Academy of Sciences, Beijing, China
- O 5 Department of Earth System Science, Tsinghua University, Beijing, China

Correspondence to: Deliang Chen (deliang@gvc.gu.se)

Abstract. Near-surface wind speed (NSWS) plays a critical role in water evaporation, air quality, and energy production. Despite its importance, NSWS changes in South Asia, a densely populated region, remain underexplored. This study aims to understand and quantify the uncertainties in the projections of NSWS over South Asia, particularly in relation to internal variability. Utilizing a 100-member large ensemble simulation from the Max Planck Institute Earth System Model, we identified the Interdecadal Pacific Oscillation (IPO) as the leading climate mode of internal variability influencing South Asian NSWS in the near future. Our findings reveal that the IPO could significantly impact future NSWS, with its positive phase being linked to strengthened westerly flows and increased NSWS across South Asia. Notably, the study shows that accounting for the impact of IPO could reduce NSWS projection uncertainty by up to 8% in the near future and 15% in the far future. This highlights the key role of internal variability, particularly the IPO, in modulating regional NSWS projections. By reducing uncertainties in these projections, our findings can inform climate adaptation strategies for South Asia, helping optimize wind energy assessments in the context of changing winds.





25 1 Introduction

Near-surface wind speed (NSWS), observed at approximately 10 meters above ground level, is a crucial meteorological variable. As a key driver in the hydrological cycle, NSWS directly impacts water evaporation and runoff (Roderick et al., 2007). Additionally, NSWS is essential for air quality management by influencing the dispersion of atmospheric pollutants (Jacobson and Kaufman, 2006). Its importance extends to the renewable energy sector, particularly in wind energy generation, where fluctuations in NSWS can significantly affect the energy output of both onshore and offshore wind farms, as highlighted by recent research (Pryor and Barthelmie, 2021; Shen et al., 2024). In 2020, wind energy contributed 6.1% of global electricity generation, with projections indicating an increase in its share as the adoption of renewable energy grows to meet international goals for carbon emissions reduction and climate change mitigation (Antonini and Caldeira, 2021; Council, 2023).

External forcings that can drive NSWS changes include greenhouse gas emissions (Zha et al., 2021; Shen et al., 2022a), aerosols (Bichet et al., 2012), volcanic eruption (Shen et al., 2025), surface roughness related to vegetation changes (Vautard et al., 2010), as well as land use and land cover change (Minola et al., 2021). Climate teleconnections such as the Atlantic Multidecadal Oscillation (AMO) (Li et al., 2024), Interdecadal Pacific Oscillation (IPO) (Shen et al., 2021a), and the North Atlantic Oscillation (Minola et al., 2016) are significant modes of internal variability. Overall, these factors can be categorized as either external forcings or internal variability drivers, and NSWS changes are driven by a combination of both (Wu et al., 2017; Zha et al., 2024).

The pressure gradient force predominantly controls changes in mean NSWS, with large-scale atmospheric circulation patterns playing a pivotal role at regional scales (Minola et al., 2023). Variations in these patterns are largely manifestations of internal variability, though external forcings like greenhouse gases and aerosols also exert some influence (Jiang and Zhou, 2023). Understanding the degree to which NSWS changes can be attributed to internal variability is essential for assessing the role of anthropogenic influences in past changes and for making reliable projections of future trends. However, current knowledge in this area remains limited.

Previous studies have investigated long-term NSWS changes over South Asia (Jaswal and Koppar, 2013; Saha et al., 2017; Das and Roy, 2024). For example, South Asian NSWS experienced a significant decline from 1961 to 2008 (Jaswal and Koppar, 2013), with a more pronounced decrease along the eastern coast compared to the western coast (Saha et al., 2017). However, only a few of these studies have attributed the observed changes to internal variability. Moreover, in model projections, NSWS shows considerable uncertainty in South Asia: Coupled Model Intercomparison Project phase 5 (CMIP5) models suggest an increase in NSWS on the eastern coast but a decrease on the western coast and northern regions by the end of the 21st century (Saha et al., 2017), while CMIP6 models project a decrease in NSWS over South Asia in the near future, followed by an increase (Shen et al., 2022a). These discrepancies emphasize the substantial uncertainties in projecting future NSWS changes over South Asia.

Distinguishing the effects of internal variability from external forcing in NSWS changes using only observational data or a single simulation is challenging, as they provide just one realization (Shen et al., 2021b). To isolate the signals of internal





variability, we utilize large-ensemble simulations (LEs). These simulations share identical greenhouse gas emission scenarios and boundary conditions but differ only in initial condition disturbances (Deser et al., 2020). The multi-member ensemble mean (MMM) of the LEs represents the effects of external forcings, while differences among members reflect the impacts of internal variability (Mitchell et al., 2017; Li et al., 2019; Wu et al., 2021). In this study, we specifically use a 100-member Max Planck Institute Earth System Model (MPI-ESM), which has been compared its historical performance with observation-based data, and applied to project NSWS changes (Zha et al., 2021; Shen et al., 2022a).

Therefore, our objectives are to (i) identify the leading mode of internal variability affecting near-future NSWS changes over South Asia and (ii) quantify the uncertainties of NSWS projections associated with internal variability. The remainder of this paper is structured as follows: Section 2 presents data and methods; Section 3 discusses the results; and the summary and discussion are provided in Section 4. These findings offer valuable insights for better understanding regional NSWS changes from the perspective of internal variability.

2 Material and Methods

2.1 Reanalysis data

70

To evaluate the ability of MPI-ESM to reproduce the historical NSWS trend over South Asia, we utilize several up-to-date reanalysis datasets. These include NSWS data from the Japanese Meteorological Agency (JRA-55) (Kobayashi et al., 2015), which is considered the most representative of observed NSWS over India (Das and Baidya Roy, 2024); the National Meteorological Information Center of the China Meteorological Administration (CRA-40) (Liu et al., 2023), which has been shown to outperform other datasets for NSWS over China (Shen et al., 2022b); and the European Centre for Medium-Range Weather Forecasts atmospheric reanalysis fifth generation (ERA5) (Hersbach et al., 2020), a global reanalysis with the highest spatial resolution (Bell et al., 2021). All reanalysis datasets cover a common period from 1970 to 2020, except for CRA-40, which spans from 1979 to 2020. To facilitate comparison, all reanalysis datasets have been bilinearly interpolated to a uniform spatial resolution of 1.5° x 1.5°.

2.2 Large-ensemble simulations

The 100-member MPI-ESM has a horizontal spatial resolution of T63 (~1.9°) and 47 vertical layers extending up to 0.01 hPa in the atmosphere. The historical simulations of MPI-ESM span from 1850 to 2005, following the protocol established within the framework of CMIP5. The representative concentration pathway scenarios, RCP4.5 and RCP8.5, with radiative forcings increasing by 4.5 W/m² and 8.5 W/m², respectively, by 2100, are performed for the period from 2006 to 2099 (Maher et al., 2019). The individual members of the MPI-ESM ensemble differ only in their initial conditions (Bittner et al., 2016), with branching times for each member from the preindustrial control run detailed in (Maher et al., 2019). These "initial condition disturbances" refer to slight variations in the starting conditions of each member, introduced to capture a range of possible outcomes driven by internal variability.

2.3 Isolating external and internal forcing signals





Considering the member discrepancies of the MPI-ESM arising from random internal variabilities, the internal variability can be isolated by the deviations in each member from the MMM:

$$A(i) = A_{forced} + A_{internal}(i), i = 1,2,3 \cdots 100$$
 (1)

where A_{forced} is the MMM of the MPI-ESM, which denotes the response to external forcings. $A_{internal}(i)$ is the residual of the original A(i) minus the external forced response. $A_{internal}(i)$ varies among different members and shows the variability associated with internal variability.

2.4 IPO and AMO definitions

The climate teleconnection index used to represent the IPO is often derived using an empirical orthogonal function (EOF) method applied to sea surface temperature (SST), as outlined by Mantua and Hare (2002b). In this study, the IPO index is defined as the 9-year running mean of the principal component (PC) score from the EOF of detrended annual SST over the North Pacific (20°N–70°N, 120°E–100°W). Similarly, the AMO index is defined as the 10-year running mean of detrended, annually averaged SST over the North Atlantic (0°N–60°N, 80°W–0°W) (Trenberth and Shea, 2006). For this analysis, both indices are calculated for each member in the LEs.

105 2.5 Quantifying the contributions of IPO/AMO to NSWS

The impacts of IPO are roughly extracted by removing the NSWS variations that are linearly related to the IPO index from 9-year running mean of NSWS, as:

$$NSWS(i,t) = r(i)_{NSWS,IPO} \times IPO(i,t) + NSWS_{non-IPO}(i,t), i = 1,2,3 \cdots 100$$
 (2)

where $r(i)_{NSWS,IPO} = \frac{\partial NSWS(i,t)}{\partial IPO(i,t)}$ is the regression coefficient of IPO index and the 9-year running mean NSWS within 110 member i during 1974–2095. Thus, $r(i)_{NSWS,PDO} \times IPO(i,t)$ represents the IPO-related component of the NSWS over South Asia in the member i and the $NSWS_{non-IPO}(i,t)$ represents the IPO-independent NSWS component without the IPO-induced variations for each member (Fig S1). Similar methods are also applied to study the contribution of AMO to NSWS. Following the timeframes selected in (Dreyfus et al., 2022), we set the 2021–2050 as the near-term and 2021–2095 as the full 21^{st} century to compare the contribution of IPO across different periods.

115



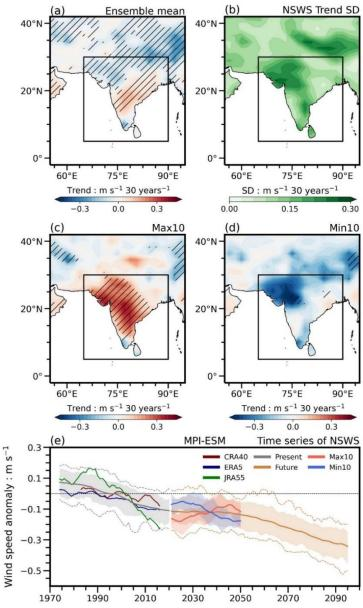


Figure 1. Temporal NSWS changes over South Asia. Annual mean near-surface wind speed (NSWS) trends under the RCP8.5 scenario for (a) the 100-member ensemble mean of MPI-ESM, (b) inter-member standard deviation, (c) the mean trend of the 10 members with the highest increase in NSWS over South Asia, and (d) the mean trend of the 10 members with the highest decline in NSWS over South Asia between 2021 and 2050. Slant hatching denotes trends that passed a significance test with P < 0.05. The box in (a) to (d) highlights the South Asia region (5°N–30°N, 65°E–90°E). (e) Time series of the 9-year running mean of NSWS anomalies (relative to the 1980–2010 mean). Purple, dark-blue, and green solid lines represent reanalysis data from CRA40, ERA5, and JRA55, respectively. Gray and brown solid lines represent the ensemble mean of all members of MPI-ESM for the present (1970–2014) and future (2015–2099), with light-gray and light-brown lines indicating the associated 5th and 95th percentiles. Orange and blue solid lines represent the ensemble mean of the ten simulations with maximum and minimum trends in NSWS. Dashed lines refer to the maximum and minimum ranges of MPI-ESM.





130

135

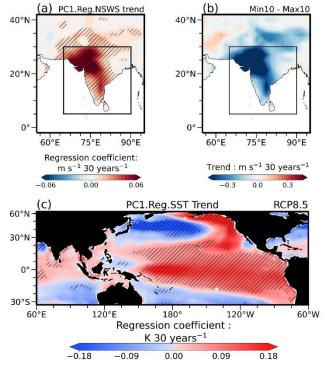
140

3 Results

3.1 Present and near-future South Asian NSWS

Under the high-emission scenario of RCP8.5, the externally forced annual NSWS in the MMM of MPI-ESM exhibits a hiatus over South Asia in the near term, reflecting inter-decadal variability. Notably, significant increases in NSWS are observed over the central and eastern coasts of India, contrasted by pronounced decreases over northern regions (Fig. 1a). The large standard deviation observed in the NSWS trends among members is comparable to the long-term trend (Fig. 1b), suggesting a substantial impact of internal variability on NSWS trends. Furthermore, the MPI-ESM successfully reproduces the current slowdown of the NSWS trend, as seen in all reanalysis datasets, with comparable magnitudes of interdecadal variability (Fig. 1e). Although the decreasing trend persists throughout the 21st century, significant uncertainty remains in near-term projections, as reflected by the large spread among members. The NSWS trends for this period range from −0.20 to 0.34 m s⁻¹ per 30 years, with the 5th to 95th percentile spread of −0.17 to 0.11 m s⁻¹ per 30 years.

To further quantify the impact of internal variability, we analyzed NSWS trends within two extreme groups: the ten members with the largest increases in NSWS (Max10) and the ten with the largest decreases (Min10). The Max10 group displays pronounced increasing trends across most of South Asia (Fig. 1c), while the Min10 group primarily exhibits significant decreasing trends over northwestern South Asia (Fig. 1d). The average trend in the Min10 and Max10 groups is -0.18 m s^{-1} per 30 years and 0.14 m s^{-1} per 30 years, respectively. The diversity in NSWS changes between these two groups, despite identical external forcing, underscores the significant role of internal variability in influencing South Asian NSWS.





150

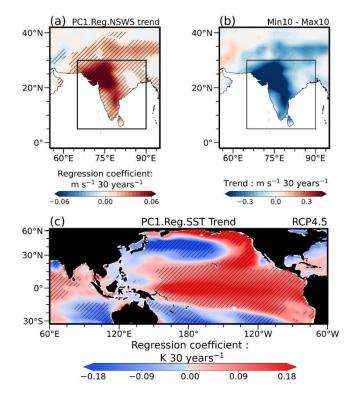
155

160



Figure 2. The leading inter-member EOF pattern of the NSWS trend over South Asia and the associated sea surface temperature trend under the RCP8.5 scenario between 2021 and 2050. (a) An EOF analysis was applied to the 100 members' NSWS trends over South Asia (5°N–30°N, 65°E–90°E) in MPI-ESM, with the member index replacing the time index in a conventional EOF analysis. (b) The group differences between the mean trend of the ten members with the highest decline in NSWS over South Asia and the ten members with the highest increase. The box in (a) and (b) highlights the South Asia region. (c) The regression pattern between the PC score and the sea surface temperature trends of corresponding members. Slashes denote regions are significant at the 95% confidence level.

To identify the leading mode of internal variability affecting NSWS and its associated SST pattern, we performed an intermember EOF analysis. As shown in Fig. 2a, NSWS exhibits a uniform enhancement across South Asia, accounting for 54.6% of the total variance. This spatial pattern closely resembles the trend differences observed between the Max10 and Min10 groups (Fig. 2b), indicating that the EOF analysis successfully captures the leading mode of NSWS variability among members. Internal climate variability stems from the non-linear dynamical processes intrinsic to the climate system, with ocean-atmosphere coupling playing a crucial role (Deser et al., 2012). The regression coefficient between the leading PC of NSWS trends and the SST trends of corresponding members from 2021 to 2050 is shown in Fig. 2c. The regression analysis reveals a significant cooling trend over the North Pacific and a significant warming trend over the tropical central-eastern Pacific, resembling a classical IPO-like mode (Mantua and Hare, 2002a). This alignment highlights the IPO's role in modulating large-scale tropical atmospheric circulation, suggesting a strong link between surface and low-level tropospheric winds over South Asia. Moreover, to assess the robustness of these findings under different warming scenarios, we compared the results from the RCP4.5 scenario with those under RCP8.5, finding that the spatial patterns are quite similar (Fig. 3).





165

170

175

180

185



Figure 3. The leading inter-member EOF pattern of the NSWS trend over South Asia and the associated sea surface temperature trend under the RCP4.5 scenario between 2021 and 2050. (a)–(c) Same as in Figure 2, but for the representative concentration pathway 4.5 (RCP4.5).

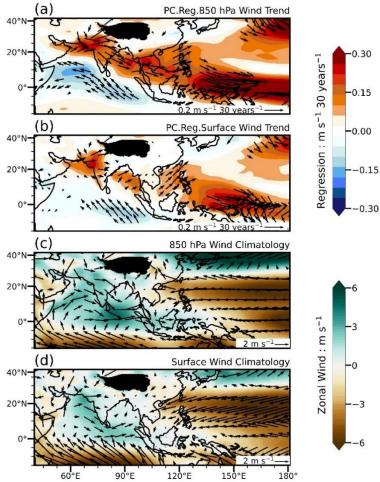
Previous works have seldom linked low-level tropospheric winds with NSWS (Wu et al. 2017). Changes in low-level

3.2 Quantifying the contribution of IPO

tropospheric winds can affect the vertical distribution of momentum, leading to changes in wind shear between different atmospheric layers (Jacobson and Kaufman, 2006). Figure 4 illustrates the regression coefficient between the leading PC of NSWS trends and the trends in winds at 850 hPa and 10m. During the positive phase of the IPO, anomalous easterly winds over the tropical Indian Ocean are observed (Fig. 4a). This anomaly in tropical oceanic low-level tropospheric winds counteracts the climatological mean state (Fig. 4b), suggesting a weakening of the Walker Circulation. The resulting anomalous descending motion triggers anticyclonic circulation to the northwest of the Maritime Continent, akin to the Gill response (Gill, 1980). The associated westerly winds, part of this anticyclone pattern near the Indian Ocean, enhance the climatological westerlies over South Asia. The MPI-ESM also provides data on surface meridional and zonal winds, allowing for exploration of the relationship between winds at 850 hPa and the surface. The spatial distributions of the regressed and climatological 10m winds (Figs. 4c and 4d) closely resemble those of the 850 hPa winds over South Asia (Figs. 4a and 4b), highlighting the consistency of atmospheric circulation changes within the region's lowest atmospheric layer. To quantify the IPO's effect on NSWS changes over South Asia in the near future, we isolated the IPO-related NSWS changes by removing the NSWS changes linearly related to the IPO index in each member (see Section 2.5). Histogram analysis reveals a narrowing in the distribution of NSWS trends over South Asia after removing the IPO's effect, with the standard deviation in the members' trends decreasing by approximately 8%, from 0.09 to 0.08 m s⁻¹ per 30 years (Fig. 5a). Although modest, these reductions suggest that the uncertainty in NSWS trend projections over South Asia could be reduced by improving our ability to predict the IPO in the future. Applying this method to far-future projections for the 21st century (2021–2095) further confirms the sensitivity of these conclusions to the selected period and underscores the significance of long-term changes, which can be compared with inter-decadal variability in the near future. As expected, by eliminating the IPO's influence, projection uncertainty is significantly reduced by 15%, nearly double the reduction observed in the near future (Fig. 5b).







190 Figure 4. Large-scale circulations associated with the inter-member EOF and climatological circulations under the RCP8.5 scenario between 2021 and 2050. (a) The regression pattern between the PC score and the trends of corresponding members' zonal wind (shading) and wind (vector) at 850 hPa. Shading and vectors denote significance at the 0.10 level. (b) Climatological zonal wind (shading) and wind (vector) at 850 hPa from 2021 to 2050 across all members of MPI-ESM. (c) Same as (a), but for winds near the surface. (d) Same as (b), but for winds near the surface.

Notably, a recent study shows that over land in Asia, projection uncertainty is mostly dominated by model uncertainty, with internal variability accounting for around 20% of the total uncertainty (Zhang and Wang, 2024). This highlights the significant role of the IPO, whose contributions of 8% and 15% represent 40% and 75% of the internal variability in different future periods, respectively. This robust quantification supports the conclusion that NSWS projections are significantly affected by the IPO, with its influence growing and extending through the end of this century.

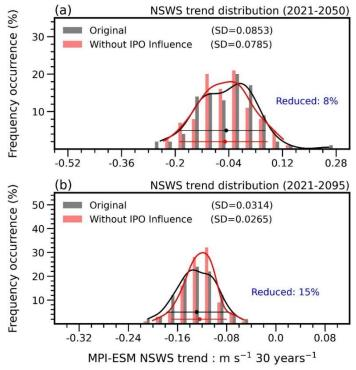


Figure 5. Histograms of the NSWS trend over South Asia in the future under the RCP8.5 scenario with and without the impact of the IPO. (a) Histograms and fitted distribution lines of the area-averaged South Asian NSWS trend derived from the 100 MPI-ESM ensemble members from 2021 to 2050. The gray bars and black fitted curves show the frequency of the occurrence of NSWS trends, while the red bars and red fitted curves represent the frequency of NSWS trends with the IPO's influence removed through linear regression against the IPO index in individual runs. (b) Same as (a), but for the period from 2021 to 2095.

4 Conclusion and Discussion

205

210

215

In this study, LEs from the MPI-ESM are used to project future changes in NSWS over South Asia. We identify the IPO as the leading mode of internal variability affecting South Asian NSWS in the near future. A positive IPO phase is conducive to enhancing westerly flows over South Asia, leading to an increase in NSWS. Furthermore, we quantify the impact of the IPO, finding that the uncertainty in NSWS projections could be reduced by approximately 8% in the near-term and 15% in the long-term after removing the IPO's effect. While these reductions may seem modest, they are crucial for regional planning, especially in wind-sensitive sectors such as energy production, agriculture, and disaster management. Our findings significantly enhance the understanding of the linkage between internal variability and regional NSWS changes. Given the substantial IPO-related uncertainty in future NSWS changes, future research should also consider other internal interdecadal climate variabilities that could impact NSWS. The AMO is another important oscillation known to influence tropical atmospheric circulation (Zhang et al., 2019). However, a similar quantification method shows that the AMO's contribution to NSWS changes is minimal, underscoring the IPO's predominance in influencing NSWS over South Asia in the near future (Fig. 6).





225

230

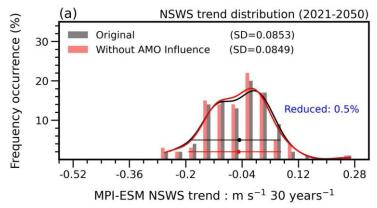


Figure 6. Histograms of the NSWS trend over South Asia under the RCP8.5 scenario with and without the impact of the AMO between 2021 and 2050. (a) Histograms and fitted distribution lines of the area-averaged South Asian NSWS trend derived from the 100 MPI-ESM ensemble members from 2021 to 2050. The gray bars and black fitted curves show the frequency of the occurrence of NSWS trends, while the red bars and red fitted curves represent the frequency of NSWS trends with the AMO's influence removed through linear regression against the AMO index in individual runs.

The resolution of the LE used may not be high enough, limiting the climate model's ability to simulate regional details of NSWS in South Asia, where the terrain is complex. There is also room for improvement in this work, which should be addressed in future research: (i) Future studies should incorporate additional LEs, with a sufficiently large ensemble size (Milinski et al., 2020), to enhance the robustness of these conclusions, which currently rely heavily on this model. (ii) The "hist-resIPO" experiment in CMIP6 historical simulations (Zhou et al., 2016), which includes all forcings used in CMIP6 historical simulations but restores SST to model climatology plus observed historical anomalies in the tropical IPO domain, could provide deeper insights into the dynamic mechanisms of IPO-related tropical SST's influence on regional NSWS changes. (iii) Future improvements in predicting the IPO, potentially achievable through the Decadal Climate Prediction Project in CMIP6 (Zhou et al., 2016), may enhance the reliability of NSWS projection over South Asia.

Additionally, future research should focus on extreme wind events against the backdrop of consistently decreasing average NSWS, especially with the background as year-maximum NSWS events are projected to increase in frequency in South Asia (Yu et al., 2024).

Financial support

This work is a contribution to the Swedish National Strategic Research Area MERGE. This work is supported by the Swedish Formas (2023-01648) and Swedish Research Council VR (2021-02163). Cheng Shen is also supported by the Sven Lindqvists Forskningsstiftelse, Stiftelsen Längmanska kulturfonden (BA24-0484) and Adlerbertska Forskningsstiftelsen (AF2024-0069). Hui-Shuang Yuan is supported by the Innovation and Entrepreneurship Training Program for College Students of Yunnan University (S202310673266). Zhi-Bo is supported by a grant from the Swedish Formas (2020-00982).





245

250

Competing interests

The contact author declares that none of the authors have any competing interests.

Author contribution

All authors reviewed and revised the manuscript. C.S. and D.C planned and designed the study. C.S and H.S.Y conducted the visualization and analysis.

Acknowledgements

This work is a contribution to the Swedish National Strategic Research Area MERGE. We would also like to express our gratitude for the insightful discussion from our colleagues in the Regional Climate Group.

Code and data availability

All datasets used in this study are publicly available. ERA5 reanalysis data is available at Hersbach et al. (2020). CRA40 reanalysis data is available at Liu et al. (2023). JRA55 reanalysis data is available at Kobayashi et al. (2015). MPI-ESM reanalysis data is available at Maher et al. (2019). The script used for generating and analyzing are available on request.





References

- Antonini, E. G. A. and Caldeira, K.: Spatial constraints in large-scale expansion of wind power plants, Proc Natl Acad Sci U S A, 118, 10.1073/pnas.2103875118, 2021.
 - Bell, B., Hersbach, H., Simmons, A., Berrisford, P., Dahlgren, P., Horányi, A., Muñoz-Sabater, J., Nicolas, J., Radu, R., and Schepers, D.: The ERA5 global reanalysis: Preliminary extension to 1950, Quarterly Journal of the Royal Meteorological Society, 147, 4186-4227, 10.1002/qj.4174, 2021.
- Bichet, A., Wild, M., Folini, D., and Schär, C.: Causes for decadal variations of wind speed over land: Sensitivity studies with a global climate model, Geophysical Research Letters, 39, 10.1029/2012GL051685, 2012.

 Bittner, M., Schmidt, H., Timmreck, C., and Sienz, F.: Using a large ensemble of simulations to assess the Northern Hemisphere stratospheric dynamical response to tropical volcanic eruptions and its uncertainty, Geophysical Research Letters, 43, 9324-9332, 10.1002/2016gl070587, 2016.
- Council, G. W. R.: Global Wind Energy, 2023.
 Das, A. and Baidya Roy, S.: JRA55 is the best reanalysis representing observed near-surface wind speeds over India, Atmospheric Research, 297, 10.1016/j.atmosres.2023.107111, 2024.
 Das, A. and Roy, S. B.: JRA55 is the best reanalysis representing observed near-surface wind speeds over India, Atmospheric Research, 297, 107111, 10.1016/j.atmosres.2023.107111, 2024.
- Deser, C., Phillips, A., Bourdette, V., and Teng, H.: Uncertainty in climate change projections: the role of internal variability, Climate dynamics, 38, 527-546, 10.1007/s00382-010-0977-x, 2012.
 Deser, C., Lehner, F., Rodgers, K. B., Ault, T., Delworth, T. L., DiNezio, P. N., Fiore, A., Frankignoul, C., Fyfe, J. C., and Horton, D. E.: Insights from Earth system model initial-condition large ensembles and future prospects, Nature Climate Change, 10, 277-286, 10.1038/s41558-020-0854-5, 2020.
- Dreyfus, G. B., Xu, Y., Shindell, D. T., Zaelke, D., and Ramanathan, V.: Mitigating climate disruption in time: A self-consistent approach for avoiding both near-term and long-term global warming, Proc Natl Acad Sci U S A, 119, e2123536119, 10.1073/pnas.2123536119, 2022.
 Gill, A. E.: Some simple solutions for heat-induced tropical circulation, Quarterly Journal of the Royal Meteorological Society, 106, 447-462, 10.1002/qj.49710644905, 1980.
- Hersbach, H., Bell, B., Berrisford, P., Hirahara, S., Horányi, A., Muñoz-Sabater, J., Nicolas, J., Peubey, C., Radu, R., and Schepers, D.: The ERA5 global reanalysis, Quarterly Journal of the Royal Meteorological Society, 146, 1999-2049, 10.1002/qj.3803, 2020.

 Jacobson, M. Z. and Kaufman, Y. J.: Wind reduction by aerosol particles, Geophysical Research Letters, 33, 10.1029/2006gl027838, 2006.
- Jaswal, A. and Koppar, A.: Climatology and trends in near-surface wind speed over India during 1961-2008, Mausam, 64, 417-436, 10.54302/mausam.v64i3.725 2013.
 Jiang, J. and Zhou, T.: Agricultural drought over water-scarce Central Asia aggravated by internal climate variability, Nature

Geoscience, 16, 154-161, 10.1038/s41561-022-01111-0, 2023.

- Kobayashi, S., Ota, Y., Harada, Y., Ebita, A., Moriya, M., Onoda, H., Onogi, K., Kamahori, H., Kobayashi, C., Endo, H., 295 Miyaoka, K., and Takahashi, K.: The JRA-55 Reanalysis: General Specifications and Basic Characteristics, Journal of the Meteorological Society of Japan. Ser. II, 93, 5-48, 10.2151/jmsj.2015-001, 2015.
 - Li, Z.-B., Xu, Y., Yuan, H.-S., Chang, Y., and Shen, C.: AMO footprint of the recent near-surface wind speed change over China, Environmental Research Letters, 19, 10.1088/1748-9326/ad7ee4, 2024.
- Li, Z., Sun, Y., Li, T., Ding, Y., and Hu, T.: Future changes in East Asian summer monsoon circulation and precipitation under 1.5 to 5 C of warming, Earth's Future, 7, 1391-1406, 10.1029/2019EF001276, 2019.
- Liu, Z., Jiang, L., Shi, C., Zhang, T., Zhou, Z., Liao, J., Yao, S., Liu, J., Wang, M., Wang, H., Liang, X., Zhang, Z., Yao, Y., Zhu, T., Chen, Z., Xu, W., Cao, L., Jiang, H., and Hu, K.: CRA-40/Atmosphere—The First-Generation Chinese Atmospheric Reanalysis (1979–2018): System Description and Performance Evaluation, Journal of Meteorological Research, 37, 1-19, 10.1007/s13351-023-2086-x, 2023.
- Maher, N., Milinski, S., Suarez-Gutierrez, L., Botzet, M., Dobrynin, M., Kornblueh, L., Kröger, J., Takano, Y., Ghosh, R., Hedemann, C., Li, C., Li, H., Manzini, E., Notz, D., Putrasahan, D., Boysen, L., Claussen, M., Ilyina, T., Olonscheck, D., Raddatz, T., Stevens, B., and Marotzke, J.: The Max Planck Institute Grand Ensemble: Enabling the Exploration of Climate





- System Variability, Journal of Advances in Modeling Earth Systems, 11, 2050-2069, 10.1029/2019ms001639, 2019.
- Mantua, N. J. and Hare, S. R.: The Pacific decadal oscillation, Journal of oceanography, 58, 35-44, 310 10.1023/A:1015820616384, 2002a.
- Mantua, N. J. and Hare, S. R.: The Pacific Decadal Oscillation, Journal of Oceanography, 58, 35-44, 10.1023/a:1015820616384, 2002b.
 - Milinski, S., Maher, N., and Olonscheck, D.: How large does a large ensemble need to be?, Earth System Dynamics, 11, 885-901, 2020.
- Minola, L., Azorin-Molina, C., and Chen, D.: Homogenization and Assessment of Observed Near-Surface Wind Speed Trends across Sweden, 1956–2013, Journal of Climate, 29, 7397-7415, 10.1175/jcli-d-15-0636.1, 2016.
 Minola, L., Reese, H., Lai, H. W., Azorin-Molina, C., Guijarro, J. A., Son, S. W., and Chen, D.: Wind stilling-reversal across Sweden: The impact of land-use and large-scale atmospheric circulation changes, International Journal of Climatology, 42, 1049-1071, 10.1002/joc.7289, 2021.
- Minola, L., Zhang, G., Ou, T., Kukulies, J., Curio, J., Guijarro, J. A., Deng, K., Azorin-Molina, C., Shen, C., Pezzoli, A., and Chen, D.: Climatology of near-surface wind speed from observational, reanalysis and high-resolution regional climate model data over the Tibetan Plateau, Climate Dynamics, 62, 933-953, 10.1007/s00382-023-06931-3, 2023.

 Mitchell, D., AchutaRao, K., and Allen, M.: Half a degree additional warming, prognosis and projected impacts (HAPPI): Background, Geoscientific Model Development, 10 (2), 10, 571-583, 10.5194/gmd-10-571-2017, 2017.
- Pryor, S. C. and Barthelmie, R. J.: A global assessment of extreme wind speeds for wind energy applications, Nature Energy, 6, 268-276, 10.1038/s41560-020-00773-7, 2021.
 - Roderick, M. L., Rotstayn, L. D., Farquhar, G. D., and Hobbins, M. T.: On the attribution of changing pan evaporation, Geophysical Research Letters, 34, 10.1029/2007gl031166, 2007.
- Saha, U., Chakraborty, R., Maitra, A., and Singh, A.: East-west coastal asymmetry in the summertime near surface wind speed and its projected change in future climate over the Indian region, Global and Planetary Change, 152, 76-87, 10.1016/j.gloplacha.2017.03.001, 2017.
 - Shen, C., Zha, J., Wu, J., and Zhao, D.: Centennial-scale variability of terrestrial near-surface wind speed over China from reanalysis, Journal of Climate, 1-52, 10.1175/jcli-d-20-0436.1, 2021a.
- Shen, C., Li, Z.-B., Liu, F., Chen, H. W., and Chen, D.: A robust reduction in near-surface wind speed after volcanic eruptions: Implications for wind energy generation, The Innovation, 6, 2025.
 - Shen, C., Li, Z. B., Yuan, H. S., Yu, Y., Lei, Y., and Chen, D.: Increases of offshore wind potential in a warming world, Geophysical Research Letters, 51, 10.1029/2024GL109494, 2024.
 - Shen, C., Zha, J., Li, Z., Azorin-Molina, C., Deng, K., Minola, L., and Chen, D.: Evaluation of global terrestrial near-surface wind speed simulated by CMIP6 models and their future projections, Annals of the New York Academy of Sciences, 1518, 249-263, 10.1111/nyas.14910, 2022a.
 - Shen, C., Zha, J., Wu, J., Zhao, D., Azorin-Molina, C., Fan, W., and Yu, Y.: Does CRA-40 outperform other reanalysis products in evaluating near-surface wind speed changes over China?, Atmospheric Research, 266, 105948, doi.org/10.1016/j.atmosres.2021.105948, 2022b.
- Shen, C., Zha, J., Zhao, D., Wu, J., Fan, W., Yang, M., and Li, Z.: Estimating centennial-scale changes in global terrestrial near-surface wind speed based on CMIP6 GCMs, Environmental Research Letters, 16, 084039, 10.1088/1748-9326/ac1378, 2021b.
 - Trenberth, K. E. and Shea, D. J.: Atlantic hurricanes and natural variability in 2005, Geophysical research letters, 33, 10.1029/2006GL026894, 2006.
- Vautard, R., Cattiaux, J., Yiou, P., Thépaut, J.-N., and Ciais, P.: Northern Hemisphere atmospheric stilling partly attributed to an increase in surface roughness, Nature Geoscience, 3, 756-761, 10.1038/ngeo979, 2010.
 - Wu, J., Zha, J., Zhao, D., and Yang, Q.: Changes in terrestrial near-surface wind speed and their possible causes: an overview, Climate Dynamics, 51, 2039-2078, 10.1007/s00382-017-3997-y, 2017.
 - Wu, M., Zhou, T., Li, C., Li, H., Chen, X., Wu, B., Zhang, W., and Zhang, L.: A very likely weakening of Pacific Walker Circulation in constrained near-future projections, Nat Commun, 12, 6502, 10.1038/s41467-021-26693-y, 2021.
- Yu, Y., Li, Z., Yan, Z., Yuan, H., and Shen, C.: Projected Emergence Seasons of Year-Maximum Near-Surface Wind Speed, Geophysical Research Letters, 51, 10.1029/2023g1107543, 2024.





- Zha, J., Chuan, T., Wu, J., Zhao, D., Luo, M., Feng, J., Fan, W., Shen, C., and Jiang, H.: Attribution of Terrestrial Near-Surface Wind Speed Changes Across China at a Centennial Scale, Geophysical Research Letters, 51, 10.1029/2024g1108241, 2024.
- Zha, J., Shen, C., Li, Z., Wu, J., Zhao, D., Fan, W., Sun, M., Azorin-Molina, C., and Deng, K.: Projected changes in global terrestrial near-surface wind speed in 1.5° C–4.0° C global warming levels, Environmental Research Letters, 16, 114016, 10.1088/1748-9326/ac2fdd, 2021.
 - Zhang, R., Sutton, R., Danabasoglu, G., Kwon, Y. O., Marsh, R., Yeager, S. G., Amrhein, D. E., and Little, C. M.: A Review of the Role of the Atlantic Meridional Overturning Circulation in Atlantic Multidecadal Variability and Associated Climate Impacts, Reviews of Geophysics, 57, 316-375, 10.1029/2019rg000644, 2019.
- Impacts, Reviews of Geophysics, 57, 316-375, 10.1029/2019rg000644, 2019.

 Zhang, Z. and Wang, K.: Quantify uncertainty in historical simulation and future projection of surface wind speed over global land and ocean, Environmental Research Letters, 19, 054029, 10.1088/1748-9326/ad3e8f, 2024.
- Zhou, T., Turner, A. G., Kinter, J. L., Wang, B., Qian, Y., Chen, X., Wu, B., Wang, B., Liu, B., Zou, L., and He, B.: GMMIP (v1.0) contribution to CMIP6: Global Monsoons Model Inter-comparison Project, Geoscientific Model Development, 9, 3589-3604, 10.5194/gmd-9-3589-2016, 2016.